View Article Online
DOI: 10.1039/C9TC03255J

COMMUNICATION

Homoconjugation enhances the photophysical and electrochemical properties of a new 3D intramolecular charge transfer iptycene displaying deep blue emission

Received 00th January 20xx,
Accepted 00th January 20xx

DOI: 10.1039/x0xx00000x

Stephanie Montanaro,[a] Daniel G. Congrave,[b] Marc K. Etherington,[c] and Iain A. Wright*[a]

A new structural class of 3D molecule capable of intramolecular charge transfer (ICT) is introduced, based upon an electron poor ring-fused triptycene core. Its photophysical and electrochemical properties are evaluated in comparison with an analogous molecule, representative of a single fin of the iptycene. Homoconjugation through the delocalised LUMO of the iptycene facilitates a great increase in transition probability both to and from the ICT state, while the deep blue photoluminescence of the single fin is retained. The peripherally distributed HOMO of the iptycene also permits reversible access to a tricationic state in a single step and at an oxidation potential lower than that of the single fin. This first example demonstrates great potential for this 3D design concept in producing new optoelectronic molecular materials.

Organic semiconductors combine interesting optoelectronic properties with the versatility of organic synthesis.[1] A facile strategy to tune their properties is to introduce intramolecular charge transfer (ICT) states through the incorporation of electron rich (donor) and electron poor (acceptor) moieties. As a result, materials with ICT characteristics have been heavily employed in organic light-emitting devices (OLEDs)[2] and organic photovoltaics (OPVs).[3] The development of compounds that improve our understanding of how to enhance and exploit ICT is, therefore, of fundamental importance to the scientific community.

Triptycene is a three-dimensional paddle-wheel type molecule[4] with a large internal free volume.[5,6] The three fused benzene "fins" of triptycene are able to communicate through the spatial overlap of their molecular orbitals, termed homoconjugation.[7,8] These properties have been broadly exploited in the development of molecular motors,[9–11] metal organic frameworks (MOFs)[12,13], porous organic crystals,[14–16] non-fullerene acceptors for OPVs[17–20] and catalysts.[21–23]

The ICT methodology has been applied to some triptycene derived compounds which are shown in Figure 1. Iptycenes have been reported with donor and acceptor fins, where ICT is facilitated through homoconjugation (Figure 1, Type A). [24–27] In some instances the relatively weak coupling afforded by homoconjugation leads to compounds exhibiting thermally activated delayed fluorescence (TADF).[24,25] This is because homoconjugation can mediate electronic communication between the HOMO and LUMO on adjacent fins, leading to a narrow singlet-triplet energy gap (ΔE_{ST}). Materials exhibiting TADF have recently received great interest, both fundamentally and as dopants in efficient next generation OLEDs.[28,29] However, emission from ICT iptycenes of this type has only been narrowly tuned between green and yellow.

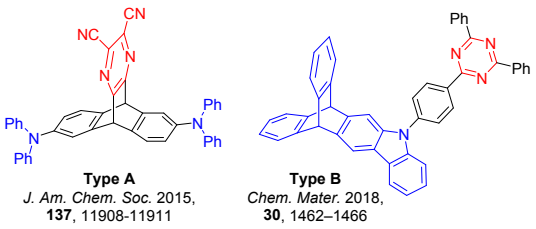

Figure 1. Chemical structures of compound **1** and representative literature ICT iptycenes.

In a second structural type (Figure 1, Type B), iptycenes have been fused onto molecules with inherent ICT characteristics.[30–32] While these systems have enabled broader colour tuning, from deep blue to orange, the effect of the iptycene is somewhat restricted to controlling intermolecular

[a] *Department of Chemistry, Loughborough University, Loughborough, Leicestershire, LE11 3TU, U.K.*
[b] *Department of Chemistry, University of Cambridge, Cambridge, CB2 1EW, U.K.*
[c] *Department of Physics, Durham University, South Road, Durham, DH1 3LE, U.K.*
† Footnotes relating to the title and/or authors should appear here.
Electronic Supplementary Information (ESI) available: [details of any supplementary information available should be included here]. See DOI: 10.1039/x0xx00000x

interactions[31] and subtly influencing the photophysical properties in comparison to their non-iptycene analogues.[32]

In this communication we introduce the donor-acceptor iptycene **1** as a new structural type (Figure 1, Type C). In **1**, pyrazine heterocycles are fused to a central triptycene core creating a trimer of quinoxaline acceptor units connected by two bridgehead sp^3 carbon atoms. Each of the quinoxalines is decorated with two 3,6-di-*tert*-butylcarbazole donors via 1,4-phenylene spacers. The photophysical and electrochemical properties of the deep blue emitter **1** were studied. To elucidate the effect of homoconjugation the single fin analogue **2** (Scheme 1) was also investigated. The beneficial properties of **2** are either retained or substantially enhanced in the iptycene **1** due to cooperation between the three fins that is facilitated by homoconjugation. This new structural type is a strong candidate for application in functional materials.

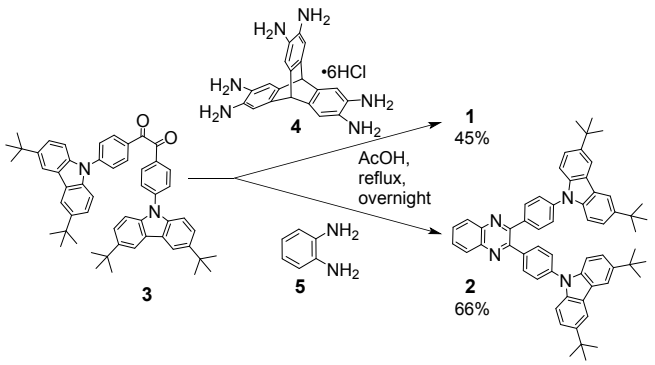

Scheme 1. Synthesis of compounds **1** and **2**.

Quinoxalines are easily and reliably synthesised through the condensation of 1,2-diketones with *ortho*-diaminobenzenes.[33] Consequently, treatment of the diketone **3** with either 2,3,6,7,14,15-hexaminotripycene hexahydrochloride[34] (**4**) or 1,2-diaminobenzene (**5**) afforded **1** and **2**, respectively (Scheme 1). Their structures and high purity were unambiguously confirmed by ^{1}H and ^{13}C NMR, mass spectrometry and elemental analyses. **1** retains the good solubility and high thermal stability (Figures S1 and S2) of **2**, which are both desirable properties for organic optoelectronic materials.

The photophysical properties of **1** and **2** were investigated in toluene solution (Figure 3, Table 1). Both molecules have three distinct bands in their absorption spectra. The sharp bands below *ca.* 350 nm are ascribed to local n–π*/ π–π* transitions on the carbazole[35] and quinoxaline[36] fragments, while the broad low energy bands are assigned to ICT.[25] The ICT band of **1** is bathochromically shifted by 19 nm compared to that of **2**. This is indicative of electronic communication between the fins, in-line with literature precedent.[7,8] The extinction coefficients for **1** are notably larger than for **2**. Specifically, we note that the ICT band is *ca.* five times as intense for **1**. This is substantially greater than the factor of three increase that would be expected in the absence of any significant electronic communication. While such an enhancement in extinction coefficient due to homoconjugation between fins is known for π–π* transitions,[7,20,37] it has not been previously employed to enhance the intensity of an ICT band, to the best of our knowledge. We note that in a non-ICT phthalimide-fused triptycene such a large increase in extinction coefficient is not observed when comparing a single fin to the iptycene.[38]

To gain a deeper insight into this phenomenon, **1** and **2** were studied by DFT/TD–DFT (B3LYP/6–31G*). HOMO and LUMO plots for **1** are shown in Figure 2. The HOMO is localised on the peripheral electron-rich *N*-phenylcarbazole fragments, while the LUMO is delocalised across the quinoxaline-triptycene core. This indicates that electronic communication between fins will be facilitated through the LUMO manifold. The frontier molecular orbital distribution for **2** is similar - the HOMO is localised across the donors and the LUMO over the quinoxaline (Figure S16).

The spectral profiles of the TD–DFT absorption spectra are in broad qualitative agreement with the experimental data (Figures S9 and S10). Unsurprisingly, due to the highly twisted structures of **1** and **2** rather narrow ΔE_{ST} values of 0.14 and 0.21 eV, respectively, are predicted. This is in agreement with experimental data for similar quinoxaline donor–acceptor compounds.[39] For **2** the ICT band consists of two near-degenerate donor–acceptor transitions with a combined oscillator strength (ƒ) of 0.1895 (Table S4), while six near-degenerate donor–acceptor transitions are predicted for iptycene **1** with a considerably increased total ƒ of 0.8819 (Table S3). These data strongly support the experimental observation of a greatly enhanced ICT absorption probability in compound **1**. Similar computational results are obtained with TDA–PBE0/def2–SVP[40] (Tables S5 and S6). Narrow ΔE_{ST} values are intrinsically associated with poor ICT oscillator strengths.[41,42] Therefore it is highly significant that compound **1** facilitates an enhancement in ICT transition probability while retaining/narrowing the calculated ΔE_{ST} of **2**. This is attributed to homoconjugation. We also note that the six lowest energy singlet states of **1** are within < 0.3 eV of T_1 and so could foreseeably contribute to enhanced emission.[42]

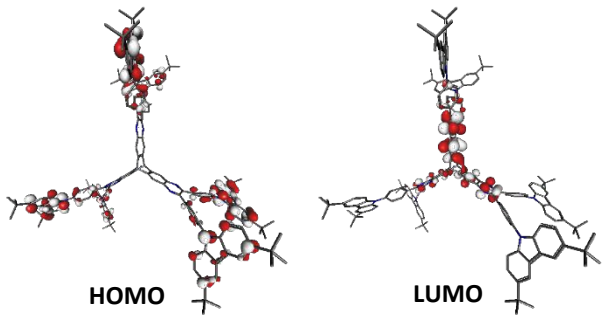

Figure 2. HOMO and LUMO plots for compound **1** from the same perspective as the chemical structure in Figure 1. Hydrogen atoms are omitted for clarity.

The PL spectra of both **1** and **2** are ascribed to ICT transitions as they are rather broad and featureless and demonstrate positive solvatochromism (Figure S3 and S4). Similarly to the absorption data, the PL (λ_{max} = 453 nm) of **1** is slightly red shifted compared to that of **2** (λ_{max} = 448 nm). This provides further

View Article Online
DOI: 10.1039/C9TC03255J

evidence of electronic communication between the fins of **1**.[7,37] We note that the Stokes shift for **1** is narrower than for **2** (51 nm vs. 65 nm), indicating that the iptycene core of **1** increases molecular rigidity. This is also expected to be responsible for the narrower PL full width at half maximum of **1** (55 nm vs. 60 nm), which beneficially results in similar deep blue Commission Internationale de L' Éclairage (CIE_{xy}) colour coordinates to **2** despite a red-shifted PL λ_{max}.

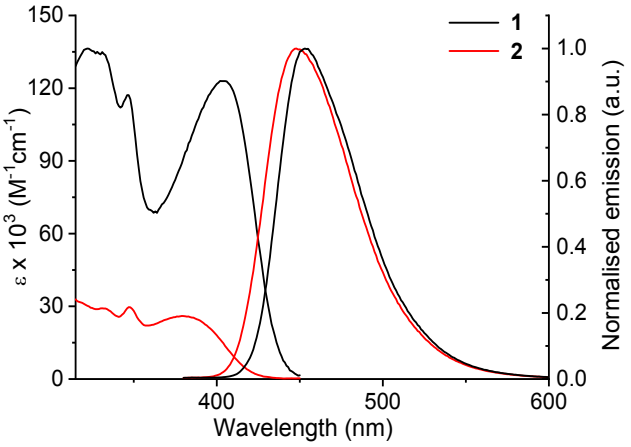

Figure 3. Absorption and emission spectra for compounds **1** and **2** recorded in toluene solution (λ_{exc} = 370 nm).

The photoluminescence quantum yield (PLQY, Φ) of **1** is significantly higher than for **2** (56% vs. 35%) while the fluorescence lifetimes (τ_F) of the two compounds are almost identical (**1** = 2.01 ns, **2** = 2.11 ns) (Table 1, Figures S5 and S6). Therefore, we can observe that the rate constants for radiative (k_r) and non-radiative (k_{nr}) decay are respectively enhanced and reduced, for **1** compared to **2**. This is in-line with the considerably higher ICT oscillator strengths observed in the absorption spectrum of **1** and calculated by TD–DFT (increase in k_r), as well as its enhanced molecular rigidity discussed above (decrease in k_{nr}). Consequently, through fusing three molecules of **2** together to create an iptycene motif (**1**), it is possible to simultaneously increase the rate of radiative decay and supress the probability of non-radiative decay while preserving highly desirable deep blue emission. Non-radiative decay is detrimental to the performance of both OLEDs and OPVs,[43,44] and so any new design concept for selectively reducing it is of great importance.

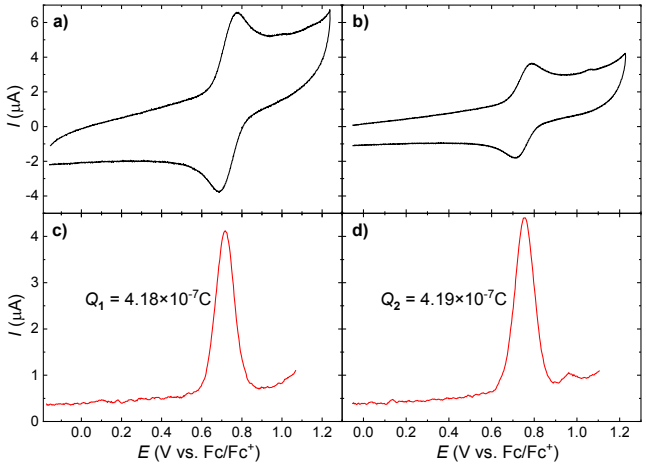

Figure 4. Cyclic voltammograms for a) **1** and b) **2** and square wave voltammograms for c) **1** and d) **2** with the total exchanged charge shown. All data were recorded in 0.1 M solutions of *n*-Bu_4NPF_6 in 1,2-dichlorobenzene.

The triplet energies of **1** and **2** were estimated from the onsets of their phosphorescence spectra recorded at 80 K for 1 wt.% doped Zeonex films (Figures S7 and S8). The triplet energy of **1** (2.48 eV) is slightly lower than that of **2** (2.56 eV) which is consistent with the trend in the singlet energies and DFT predictions (Tables S3–S6). The experimentally obtained ΔE_{ST} for **1** (0.49 eV) is also slightly smaller than for **2** (0.54 eV). This is also consistent with DFT predictions (Tables S3–S6), although the experimental ΔE_{ST} values are somewhat larger. Nevertheless, through our design strategy it appears to be possible to desirably enhance both the absorption to, and emission from an ICT state in a deep blue compound, without increasing the ΔE_{ST}. Future work should focus on applying this strategy to narrower ΔE_{ST} materials.[41,42]

The photophysical benefits of the electron poor 3D core of **1** over the single fin **2** can all be ascribed to homoconjugation through the LUMO manifold. To understand the influence of this highly symmetric 3D structure and the implications of having six rather than two donor moieties on the behaviour of the HOMO manifold, cyclic voltammetry (CV) and square wave voltammetry (SWV) experiments were performed on 1,2-dichlorobenzene solutions of **1** and **2**. Results are shown in Figure 4 and summarised in Table 1.

Table 1. Photophysical and electrochemical data for compounds **1** and **2**.

	λ_{abs} / nm [ε × 10^3 M^{-1} cm^{-1}]	$\lambda_{max\ PL}$ / nm [CIE_{xy}]	Φ /%[a]	τ_F / ns[b]	k_r / × 10^8 s^{-1}	k_{nr} / × 10^8 s^{-1}	ΔE_{ST} / eV [S_1/T_1][c]	E_{ox} / V	$\Delta E_{1/2}$ / mV	E_{red} / V	HOMO[d] / eV	LUMO[d] / eV	E_g / eV
1	322 [136], 346 [117], 402 [123]	453 [0.14, 0.11]	56, 51	2.01	2.65	2.09	0.49 [2.97/2.48]	+0.73	100	Not obs.	−5.73	-	
2	331 [29], 347 [30], 383 [26]	448 [0.15, 0.09]	35, 33	2.11	1.74	3.23	0.54 [3.10/2.56]	+0.75	80	−2.12	−5.76	−2.89	2.87

Absorption and emission data were recorded in toluene. Electrochemical data were obtained in degassed 0.1 M *n*-Bu_4PF_6 in dichlorobenzene. [a]Order of measured values is degassed followed by air equilibrated. Determined vs. quinine sulfate in 0.1 M H_2SO_4 as standard (Φ = 0.546), error is 5% or better. [b]Error is ± 0.05 ns. $\tau_F = 1/k_r + k_{nr}$ [c]Singlet-triplet energy splitting and singlet/triplet energies measured in Zeonex 1 wt%. [d]HOMO and LUMO levels calculated from the onset of the first oxidation and reduction waves respectively and are referenced the HOMO of ferrocene at −5.10 eV. [e]Electrochemical HOMO–LUMO gap.

DOI: 10.1039/C9TC03255J

The CV of both **1** and **2** display a single electrochemically reversible oxidation process at +0.73 V and +0.75 V vs. Fc/ Fc^+, respectively, arising from oxidation of the electron rich carbazole rings. This indicates that the iptycene core in **1** has little impact on the HOMO energy compared to the simple quinoxaline in **2**, in agreement with the almost equivalent HOMO energies predicted for **1** and **2** by DFT (Figures S15 and S16). In the SWV of accurately prepared 0.1 mg mL^{-1} solutions the magnitude of the exchanged charge (calculated by integrating the oxidation wave) was near identical (Q_1/Q_2 = 0.998) for **1** and **2**. Correcting for the three-fold increase in molecular weight of **1** compared to **2**, and thereby the three-fold lower molarity of the solution of **1**, this result demonstrates that at a slightly lower potential three times as many electrons are lost from the iptycene compound **1** as from the single fin quinoxaline **2**.

To further quantify this, ferrocene was used as a coulometric standard[45] taking advantage of its ability to undergo a fully reversible single-electron oxidation. A solution containing equimolar quantities of ferrocene and **2** was subject to SWV and integration of the waves revealed that the exchanged charge was near identical for both species (Q_2/Q_{Fc} = 0.999, Figure S17). This confirms that **2** is a single electron donor and, consequently, that **1** is a three-electron donor that can be reversibly oxidised to have a radical cation localised on each fin of the molecule at a single oxidation potential. The perfectly overlapped and reversible structure of the oxidation wave indicates that there are no coulombic interactions between the carbazole rings of each fin.[20,37]

At negative potentials no reduction process was apparent in the CV of iptycene **1** but, interestingly, the quinoxaline **2** showed an irreversible single-electron reduction on the edge of the accessible solvent window at –2.12 V vs. Fc/Fc^+ (Figure S18). DFT predicts a more negative LUMO energy for **1** vs. **2** (Figures S11 and S12) and **1** has a narrower optical energy gap (Figure 3). Therefore, we suggest that for **1** the steric bulk of the pendant 3,6-di-*tert*-butyl-carbazole groups physically shields the quinoxalines from the electrode surface, thereby increasing the potential energy barrier towards electron transfer and reduction. In this way the iptycene core has also stabilised the molecule against reductive degradation.

In conclusion, we have introduced compound **1** as a new structural type of ICT iptycene. In our new design the fine balance of electronic communication between the three donor–acceptor fins is crucial. This communication, afforded by homoconjugation, occurs through the LUMO manifold but not via the peripheral donors (through the HOMO). As a result, the three fins in **1** behave independently enough that they participate in a three-electron oxidation. Simultaneously, the inter-fin communication is adequate to facilitate a great increase in transition probability both to and from the ICT state, which has not been previously exploited. This is particularly noteworthy because **1** features a narrower ΔE_{ST} than **2** - increasing the ICT oscillator strength in such compounds while narrowing ΔE_{ST} is an established and fundamental problem.[46] **1** also retains the deep blue emission of **2** due to the high rigidity of its iptycene core. These results should be of broad interest when developing new functional materials for applications reliant on CT states, such as OLEDs and OPVs.

Conflicts of interest

There are no conflicts to declare.

Acknowledgements

I. A. W. thanks Loughborough University for support and the Royal Society of Chemistry Research Fund (RF18-5353) for funding. I. A. W. also thanks the Durham University Mass Spectrometry Service for ASAP-MS and MALDI-TOF MS. S. M. acknowledges Loughborough University for providing a PhD studentship. M.K.E. acknowledges the EU's Horizon 2020 research and innovation programme for funding the HyperOLED project under grant agreement No. 732013. We would like to thank A.P. Monkman and F.B. Dias for providing access to their experimental setups. Sandra Dressler is thanked for running TGA analyses.

References

1 S. R. Forrest and M. E. Thompson, *Chem. Rev.*, 2007, **107**, 923–925.

2 W. Z. Yuan, Y. Gong, S. Chen, X. Y. Shen, J. W. Y. Lam, P. Lu, Y. Lu, Z. Wang, R. Hu, N. Xie, H. S. Kwok, Y. Zhang, J. Z. Sun and B. Z. Tang, *Chem. Mater.*, 2012, **24**, 1518–1528.

3 K. Tvingstedt, K. Vandewal, A. Gadisa and F. Zhang, *J. Am. Chem. Soc.*, 2009, **131**, 11819–11824.

4 P. D. Bartlett, M. J. Ryan and S. G. Cohen, *J. Am. Chem. Soc.*, 1942, **64**, 2649–2653.

5 N. T. Tsui, A. J. Paraskos, L. Torun, T. M. Swager and E. L. Thomas, *Macromolecules*, 2006, **39**, 3350–3358.

6 T. M. Swager, *ChemInform*, 2008, **39**, 1181–1189.

7 T. Kodama, Y. Hirao, T. Nishiuchi and T. Kubo, *Chempluschem*, 2017, **82**, 1006–1009.

8 T. Kodama, S. Miyazaki and T. Kubo, *Chempluschem*, 2019, **84**, 1–5.

9 T. R. Kelly, H. De Silva and R. A. Silva, *Nature*, 1999, **401**, 150–152.

10 X. Z. Zhu and C. F. Chen, *J. Am. Chem. Soc.*, 2005, **127**, 13158–13159.

11 D. K. Frantz, A. Linden, K. K. Baldridge and J. S. Siegel, *J. Am. Chem. Soc.*, 2012, **134**, 1528–1535.

12 A. K. Crane, B. O. Patrick and M. J. MacLachlan, *Dalt. Trans.*, 2013, **42**, 8026–8033.

13 A. K. Crane, E. Y. L. Wong and M. J. MacLachlan, *CrystEngComm*, 2013, **15**, 9811–9819.

14 M. Mastalerz and I. M. Oppel, *Angew. Chemie - Int. Ed.*, 2012, **51**, 5252–5255.

15 J. H. Chong, S. J. Ardakani, K. J. Smith and M. J. MacLachlan, *Chem. - A Eur. J.*, 2009, **15**, 11824–11828.

16 B. S. Ghanem, M. Hashem, K. D. M. Harris, K. J. Msayib, M. Xu, P. M. Budd, N. Chaukura, D. Book, S. Tedds, A. Walton and N. B. McKeown, *Macromolecules*, 2010, **43**, 5287–5294.

17 Y. Zhang, B. Kan, X. Ke, Y. Wang, H. Feng, H. Zhang, C. Li, X. Wan and Y. Chen, *Org. Electron.*, 2017, **50**, 458–465.

18 S. M. Menke, N. A. Ran, G. C. Bazan and R. H. Friend, *Joule*, 2018, **2**, 25–35.

19 E. H. Menke, V. Lami, Y. Vaynzof and M. Mastalerz, *Chem. Commun.*, 2016, **52**, 1048–1051.

20 S. R. Peurifoy, E. Castro, F. Liu, X. Y. Zhu, F. Ng, S. Jockusch, M. L. Steigerwald, L. Echegoyen, C. Nuckolls and T. J. Sisto, *J. Am. Chem. Soc.*, 2018, **140**, 9341–9345.

21 O. Grossman and D. Gelman, *Org. Lett.*, 2006, **8**, 1189–1191.

22 S. Gonell, M. Poyatos and E. Peris, *Angew. Chemie - Int. Ed.*, 2013, **52**, 7009–7013.

23 C. Azerraf, S. Cohen and D. Gelman, *Inorg. Chem.*, 2006, **45**, 7010–7017.

24 K. Kawasumi, T. Wu, T. Zhu, H. S. Chae, T. Van Voorhis, M. A. Baldo and T. M. Swager, *J. Am. Chem. Soc.*, 2015, **137**, 11908–11911.

25 C. C. A. Voll, J. U. Engelhart, M. Einzinger, M. A. Baldo and T. M. Swager, *European J. Org. Chem.*, 2017, **2017**, 4846–4851.

26 Y. Gao, T. Su, Y. Wu, Y. Geng, M. Zhang and Z. M. Su, *Chem. Phys. Lett.*, 2016, **666**, 7–12.

27 R. Qian, H. Tong, C. Huang, J. Li, Y. Tang, R. Wang, K. Lou and W. Wang, *Org. Biomol. Chem.*, 2016, **14**, 5007–5011.

28 Y. Liu, C. Li, Z. Ren, S. Yan and M. R. Bryce, *Nat. Rev. Mater.*, 2018, **3**, 18020.

29 Y. Liu, C. Li, Z. Ren, S. Yan and M. R. Bryce, *Nat. Rev. Mater.*, 2018, **3**, 1605444.

30 A. L. Schleper, C. C. A. Voll, J. U. Engelhart and T. M. Swager, *Synlett*, 2017, **28**, 2783–2789.

31 T. Kang, H. Kim and D. Lee, *Org. Lett.*, 2017, **19**, 6380–6383.

32 W. Huang, M. Einzinger, T. Zhu, H. S. Chae, S. Jeon, S.-G. Ihn, M. Sim, S. Kim, M. Su, G. Teverovskiy, T. Wu, T. Van Voorhis, T. M. Swager, M. A. Baldo and S. L. Buchwald, *Chem. Mater.*, 2018, **30**, 1462–1466.

33 M. Tingoli, M. Mazzella, B. Panunzi and A. Tuzi, *European J. Org. Chem.*, 2011, 399–404.

34 M. G. Rabbani, T. E. Reich, R. M. Kassab, K. T. Jackson and H. M. El-Kaderi, *Chem. Commun.*, 2012, **48**, 1141–1143.

35 Z. Wei, J. Xu, G. Nie, Y. Du and S. Pu, *J. Electroanal. Chem.*, 2006, **589**, 112–119.

36 R. C. Hirt, F. T. King and J. C. Cavagnol, *J. Chem. Phys.*, 1956, **25**, 574–576.

37 L. Lv, J. Roberts, C. Xiao, Z. Jia, W. Jiang, G. Zhang, C. Risko and L. Zhang, *Chem. Sci.*, 2019, **10**, 4951–4958.

38 D. Wu, H. Zhang, S. H. Liu and J. Yin, *Chem. - An Asian J.*, 2015, **10**, 602–607.

39 R. Pashazadeh, P. Pander, A. Lazauskas, F. B. Dias and J. V. Grazulevicius, *J. Phys. Chem. Lett.*, 2018, **9**, 1172–1177.

40 M. Moral, L. Muccioli, W. Son, Y. Olivier and J. C. Sancho-Garcia, *J. Chem. Theory Comput.*, 2015, **11**, 168–177.

41 A. Pershin, D. Hall, V. Lemaur, J. C. Sancho-Garcia, L. Muccioli, E. Zysman-Colman, D. Beljonne and Y. Olivier, *Nat. Commun.*, 2019, **10**, 597.

42 P. L. dos Santos, J. S. Ward, D. G. Congrave, A. S. Batsanov, J. Eng, J. E. Stacey, T. J. Penfold, A. P. Monkman and M. R. Bryce, *Adv. Sci.*, 2018, **5**, 1700989–1700998.

43 J. Benduhn, K. Tvingstedt, F. Piersimoni, S. Ullbrich, Y. Fan, M. Tropiano, K. A. McGarry, O. Zeika, M. K. Riede, C. J. Douglas, S. Barlow, S. R. Marder, D. Neher, D. Spoltore and K. Vandewal, *Nat. Energy*, 2017, **2**, 17053.

44 S. Ullbrich, J. Benduhn, X. Jia, V. C. Nikolis, K. Tvingstedt, F. Piersimoni, S. Roland, Y. Liu, J. Wu, A. Fischer, D. Neher, S. Reineke, D. Spoltore and K. Vandewal, *Nat. Mater.*, 2019, **18**, 459–464.

45 S. Krykun, V. Croué, M. Allain, Z. Voitenko, J. Aragó, E. Ortí, S. Goeb and M. Sallé, *J. Mater. Chem. C*, 2018, **6**, 13190–13196.

46 X. K. Chen, Y. Tsuchiya, Y. Ishikawa, C. Zhong, C. Adachi and J. L. Brédas, *Adv. Mater.*, 2017, **29**, 1702767.

View Article Online
DOI: 10.1039/C9TC03255J

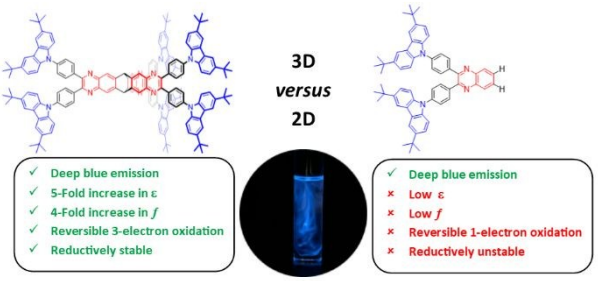

Greater than the sum of its parts – a 3D ICT molecule displays greatly improved optoelectronic properties over a 2D analogue.